X-691-77-37

PREPRINT

TMX 71304

PERFORMANCE CHARACTERISTICS OF A THREE-AXIS SUPERCONDUCTING ROCK MAGNETOMETER

BARRY R. LIENERT

FEBRUARY 1977

GSFC

GODDARD SPACE FLIGHT CENTER

GREENBELT, MARYLAND

PERFORMANCE CHARACTERISTICS OF A THREE-AXIS SUPERCONDUCTING ROCK MAGNETOMETER

*Barry R. Lienert

*Astrochemistry Branch
NASA/Goddard Space Flight Center
Greenbelt, Maryland

ABSTRACT

A series of measurements have been carried out with the purpose of quantitatively determining the characteristics of a commercial 6.8 cm access superconducting rock magnetometer located in the magnetic properties laboratory at the Goddard Space Flight Center. The measurements have shown that although a considerable improvement in measurement speed and signal to noise ratios can be obtained using such an instrument, a number of precautions are necessary to obtain accuracies comparable with more conventional magnetometers. These include careful calibration of the sensor outputs, optimum positioning of the sample within the detection region and quantitatively establishing the degree of cross-coupling between the detector coils. In order to examine the uniformity of response for each detector, the responses have been mapped as a function of position, using a small dipole. The response variations were found to be less than 5% within an optimally positioned cylinder 2.5 cm in diameter and 4 cm in length. With the application of suitable correction terms, the magnetization of a 2.5 cm diameter core sample can be determined to an angular accuracy of better than half a degree, using a single insertion of the sample. For smaller diameter access magnetometers, spatial variation of the coil response characteristics will be more significant requiring repeated measurements of inhomogeneous samples in different orientations to average out the resulting errors.

INTRODUCTION

Superconducting rock magnetometers have, in the last few years, come from being something of a scientific curiosity, to a standard instrument used in paleomagnetic and rock magnetic research. The reason for this is their capability of measuring weakly magnetized rocks, such as oceanic sediments, very rapidly. Their principles of operation and various applications have been described by Goree and Fuller (1976).

Although large quantities of data have now been obtained using this type of magnetometer, no detailed assessment of its operational characteristics has so far been published. Very little information has been provided by the manufacturers on such important details as alignment accuracy of the detector coils and the spatial uniformity of their response characteristics. In this paper I shall describe a series of tests run on an instrument in operation at NASA/Goddard Space Flight Center. This instrument is of similar design to almost all the superconducting magnetometers presently in use.

DESCRIPTION OF THE INSTRUMENT

Figure 1 is a schematic showing the position of the single loop sense coils relative to the sample access, which in this instrument has a diameter of 6.8cm. The coils and sensors are surrounded by a superconducting lead shield which has the capability of "freezing in" the field in which it is allowed to cool below the shield transition temperature.

It is clear from Figure 1 that only the vertical axis coil is of the true Helmholtz design, the two horizontal coils having a rectangular shape which in turn is curved around the dewar wall. Additional shielding is used above and below the detector coils to ensure the sample moment only couples with the coils within a limited region. In this way a zero reading can be taken with the sample only a small distance away from the detection region. The outputs of each coil sensor are calibrated by the manufacturers who use a small solenoid whose equivalent moment is known.

Since each coil measures the total (remanent plus induced) moment, along each axis, it is necessary to make remanent moment measurements in a low field. How large a field can be tolerated depends on the magnetic characteristics of the samples being measured. In practice, a field smaller than 20 nT is usually found to be satisfactory. In this study, the maximum magnetic field within the detection region was less than 10 nT. The field gradients were less than 1 nT/cm (1 nT = 10^{-5} gauss = 1 gamma).

RESPONSE OF THE DETECTOR COILS

The spatial variation of the output of each of the three axes was checked using a small (1mm diameter) sample, which was given a saturation moment along one of its axes. Profiles of output versus vertical position were then obtained for each of the twelve horizontal positions shown in Figure 2. These profiles are shown in Figure 3. The sample was oriented so that its moment was along the axis being tested in each case. The figures adjacent to each profile represent the value of the output (in arbitrary units) at the midpoint of each profile.

The results indicate that the region within which the response is uniform to within a few percent is fairly limited. The vertical axis defines the minimum volume of uniform response, which is a cylinder approximately 4 cm long and 2.5 cm in diameter, within which the variation in output is less than 5%.

The horizontal axes responses are similarly uniform within a larger volume - a cylinder about 6 cm long and 3 cm in diameter. Although these volumes include the standard 2.5 cm diameter cores used in most paleomagnetic studies, it must be emphasized that these results are for a 6.8 cm access instrument. For the more common 3.8 cm access instrument, the volume of uniform response would be correspondingly smaller, and almost certainly less than the standard core volume. The amount of error that this would cause in a single measurement would depend on the degree of inhomogeneity in the sample being measured. However, it is clear that significant errors could be introduced in this fashion.

CALIBRATION PROCEDURES:

Absolute Calibrations were made using a small (0.476 cm diameter) 5 turn coil. The equivalent dipole moment of this coil was taken as

$$M = nIA/10 \text{ emu}$$

where A is the area of the coil in cm^2, n is the number of turns and I is the current in amperes.

The coil was positioned at the mid-point of the vertical response profile shown in Figure 3 (Z) and the current varied by an amount corresponding to 10^{-4} emu (1.12 mA). The calibration potentiometers in the magnetometer electronics were then adjusted to give corresponding changes in the magnetometer readouts of 10^{-4} emu, with the coil oriented along each axis in turn. The calibrations agreed to within a few percent with those performed by the manufacturers with the exception of the X sensor, which had recently been replaced and not subsequently recalibrated.

Goree and Fuller (1976) have reported significant non-linearities in the output of their instrument. Linearity was therefore checked on the x10 range by plotting magnetometer output versus coil current, with the coil. The results indicated that linearity was better than 0.5% for all three axes. The experiment was also repeated for the X100 range with similar results.

AXIS ORIENTATIONS

The effective orientation of each axis was checked using a sample with most of its moment directed along a single axis. The direction of the major moment was then positioned at ten degree intervals in a plane at right angles to the axis being tested. In this way, cross-coupling effects show up as a variation in the output of the axis being tested, which should remain constant if the axes are truly orthogonal. The results are shown in Figure 4 (a), (b), and (c). They indicate small amounts (about 1%) of cross coupling between all three axes. Since the variations are approximately sinusoidal, it should be possible to correct for these effects using cross coupling coefficients whose values are known. If the true values of the three orthogonal components in the sample are X, Y, Z and the observed values X^1, Y^1, Z^1, then

$$X^1 = X + C_{yx}Y + C_{zx}Z \quad (1)$$

$$Y^1 = Y + C_{xy}X + C_{zy}Z \quad (2)$$

$$Z^1 = Z + C_{xz}X + C_{yz}Z \quad (3)$$

The cross-coupling terms C_{xy}, C_{xz} ... can be estimated from the plots in Figure 4. However, a more convenient way to estimate them is to measure a calibration sample in different orientations. The calculations are considerably simplified if the calibration sample has most of its moment along one axis, as each cross-coupling term can then be estimated independently. Two measurements are then required for each cross coupling term. For example, to obtain C_{yx}, the major moment of the sample is oriented along the Y axis, and the value

X^1 measured. The Y and Z components are then inverted by rotating the sample 180^o about its X axis and a second value of X^1 obtained. It then follows from equation (1) that the difference between the first and second values of X^1 will be $2C_{yx}Y$, provided the last term, $C_{zx}Z$, is assumed negligible in both instances. If Y^1 is assumed equal to Y, the coefficient C_{yx} can then be obtained. A more complete determination of the coefficients can be made using appropriate measurements on any sample at all. However, this will clearly involve inversion of a matrix which the above method avoids.

Shown in Table 1 are the results of measurements of a calibration sample with its cubical sample holder oriented in all possible (24) positions relative to the magnetometer measuring axes. This data can be used to obtain four independent estimates of each cross coupling term by suitably combining the data in the manner already described. The average values of the cross-coupling terms so obtained also appear in Table 1. The additional terms C_{xx}, C_{yy}, and C_{zz} are calibration normalisation terms. These were calculated by averaging all the measurements of the main component of magnetization for each axis, then normalising the results to the average value for the Z axis. In this way, calibration errors between the three axes are corrected for. The results of applying the corrections according to equations (1), (2), and (3) appear in Table 2. It is apparent that the scatter in the results has been reduced from almost 2^o to less than 0.2^o. Tables 3 and 4 show the results of similar measurements on a 2.5 cm diameter core of fine-grained basalt. Again, a considerable reduction in the scatter of the results is evident.

This reduction in scatter can be more easily seen in Figure 6, which shows plots of inclination versus declination before and after correction for cross-coupling for the basalt sample. The slightly larger scatter of the corrected results in Table 4 (about 0.5^{o}) is probably due to the larger size of this sample compared to the original calibration sample, which was only ~ 2 mm in diameter and 2 mm in length. The directional variation may therefore be due to small inhomogeneities in the rock sample causing differences in the coil responses as outlined in the previous section.

One interesting feature of the cross coupling coefficients shown in Table 1 is that, for example, C_{xy} is not the same as C_{yx}. This implies that the coupling cannot simply be attributed to misalignment of the coils, for this would clearly imply that these two terms should be equal. Some of the coupling is probably between the wires leading up to each coil and the other coils. This would explain the non-commutative behavior of the coupling terms.

NOISE MEASUREMENTS

Shown in Figure 5 are output traces recorded over a 5 minute period using the 1hz bandwidth filter. The traces also show deflections recorded for insertion of samples having the indicated moments. The short term noise varies from about 2×10^{-8} emu r.m.s. for the x axis to 1×10^{-8} emu r.m.s. for the Z axis. The long term drift ranges from 5×10^{-9} emu/min for the Z axis to 2×10^{-8} emu/min for the Y axis. The larger drift in the horizontal sensor outputs seemed to be related to less effective shielding in the horizontal directions. It was found experimentally that a magnet producing 10 gauss at the sense coils caused a change of 10^{-5} emu in the outputs of the horizontal sensors. This implied that field changes of 0.01 gauss, which are fairly common in urban evnironments can cause observable noise in these magneto-meters outputs. The vertical shielding factor is much greater - the 10 gauss magnet produced no observable change in the output of the vertical sensor.

DISCUSSION

Superconducting magnetometers of this type are clearly useful instruments for measuring weak magnetization in paleomagnetic samples. Although their spatial response characteristics are clearly more uniform than those of either spinner magnetometer coils or fluxgates, significant variations are nevertheless present.

To eliminate the effect of these, measurements need to be performed with samples in different orientations and the results averaged as has been done with spinner magnetometer data. It has been shown that with suitable precautions, a one-inch diameter core can be measured with a single insertion to an angular accuracy of better than 0.5^{o}. However, with a 3.8 cm access instrument, the angular error could be much greater.

REFERENCES

Goree, W. S. and Fuller, M., "Magnetometers using RF driven SQUIDS and their applications in rock magnetism and paleomagnetism" Rev. Geophys. Sp. Phys. v. 14, No. 4, pp. 591-608, 1976.

TABLES

Table 1 - Measurements of calibration sample in different orientations. Also shown are the cross coupling terms calculated from this set of measurements using the methods described in the text.

Table 2 - Corrected calibration sample measurements. Note the large reduction in scatter compared to Table 1.

Table 3 - Measurements similar to those in Table 1, for a 2.5 cm diameter core of fine grained basalt.

Table 4 - Corrected results for the basalt core.

FIGURE CAPTIONS

Figure 1 - Sense coil geometry for a two-axis system.

Figure 2 - Horizontal positions of response profiles. The numbers in the circles correspond to the numbers on the left hand side of each of the profiles in Figure 3.

Figure 3 - Response of each axis to a sample as a function of vertical position in each of the positions defined in Figure 2. The numbers at the center of each profile are the output moment values (arbitrary units) at the optimum position defined by the vertical responses. (See text)

Figure 4 - Cross coupling response for: (a) the X axis, (b) the Y axis and (c) the Z axis. The upper two curves in each case are the variations in output of two of the axes when the sample is rotated about the third axis. The lower curve is the variation in the response of this third axis, which for no cross coupling, should be zero.

Figure 5 - Noise measurements made over 5 to 7 minute periods (not synchronously) for each axis. Also shown is the effect of inserting the small moments indicated, into the sense region.

Figure 6 - Plots of inclination, versus declination for the basalt core as measured in all 24 orientations, before and after correction for cross-coupling effects.

X	Y	Z	D	I	M
38.1200	2.0400	0.0700	86.93	0.10	0.3817E-01
0.0400	2.0500	-37.7900	86.89	0.06	0.3784E-01
-38.0700	2.0600	0.0400	86.90	-0.06	0.3812E-01
0.0000	1.8700	37.7800	87.16	0.00	0.3782E-01
38.1400	-0.3200	1.4800	87.77	0.48	0.3817E-01
38.1800	0.2800	-2.1400	86.79	0.41	0.3824E-01
-1.2100	38.3400	0.6200	88.19	0.92	0.3836E-01
1.0100	38.2800	2.1600	86.77	1.50	0.3835E-01
2.4300	38.2600	0.0000	86.36	0.00	0.3833E-01
0.2800	38.3100	-1.5200	87.72	-0.41	0.3834E-01
-1.5200	-0.4000	37.8600	87.70	0.60	0.3789E-01
-2.1800	0.3900	-37.7500	86.69	0.59	0.3781E-01
-38.1700	-1.9000	0.5700	87.15	0.85	0.3822E-01
0.6400	-2.0300	37.8200	86.92	0.96	0.3787E-01
38.1300	-2.0500	-0.6900	86.92	1.03	0.3819E-01
-0.6700	-1.8600	-37.7100	87.17	1.01	0.3776E-01
-38.1000	-0.2300	-1.6100	87.58	0.34	0.3813E-01
-38.1000	0.4300	2.2000	86.69	0.64	0.3816E-01
1.2400	-38.1800	0.1200	88.14	0.17	0.3820E-01
-0.3700	-38.1600	-2.1100	86.83	-0.55	0.3822E-01
-2.5700	-38.1700	-0.5500	86.14	0.82	0.3826E-01
-0.9400	-38.1500	1.5700	87.64	1.41	0.3819E-01
1.4700	-0.2400	-37.7400	87.76	0.36	0.3776E-01
2.1700	0.3300	37.6400	86.70	0.50	0.3770E-01

C_{xx} = .9904	C_{yx} = 0.0169	C_{zx} = 0.0086
C_{xy} = 0.0013	C_{yy} = 0.9877	C_{zy} = 0.0019
C_{xz} =-0.0082	C_{yz} = 0.0074	C_{zz} = 1.0000

X, Y, Z - Magnetometer outputs for each axis

D, I - Declination, inclination relative to sample

M - Total moment (x 10^{-4} emu)

Table 1: Measurements of calibration sample in different orientations

X	Y	Z	D	I	M
37.7199	2.0656	0.3644	86.86	0.55	0.3777E-01
0.3308	1.9548	-37.8017	87.04	0.50	0.3785E-01
-37.7406	1.9841	-0.2844	86.99	0.43	0.3779E-01
-0.3573	1.9169	37.7629	87.09	0.54	0.3781E-01
37.7675	-0.2626	1.7919	87.28	0.39	0.3781E-01
37.8281	0.3232	-1.8318	87.22	0.48	0.3787E-01
-1.8511	37.8673	0.3252	87.20	0.49	0.3791E-01
0.3353	37.8183	1.8836	87.14	0.50	0.3786E-01
1.7607	37.7919	-0.2645	87.33	0.40	0.3783E-01
-0.3564	37.8357	-1.8022	87.27	0.53	0.3788E-01
-1.8251	-0.3269	37.8474	87.23	0.49	0.3789E-01
-1.8402	0.3123	-37.7674	87.21	0.47	0.3781E-01
-37.7774	-1.9262	0.2740	87.08	0.41	0.3782E-01
0.3420	-1.9341	37.8370	87.07	0.51	0.3788E-01
37.8055	-1.9754	-0.3650	87.00	0.55	0.3785E-01
-0.3070	-1.9078	-37.6984	87.10	0.46	0.3774E-01
-37.7174	-0.2807	-1.9175	87.08	0.42	0.3776E-01
-37.7614	0.3781	1.8872	87.13	0.57	0.3781E-01
1.8717	-37.7078	0.4137	87.15	0.62	0.3775E-01
0.2960	-37.6944	-1.8293	87.22	0.44	0.3773E-01
-1.8961	-37.7043	-0.2872	87.12	0.43	0.3775E-01
-0.3003	-37.6784	1.8456	87.19	0.45	0.3772E-01
1.7853	-0.3049	-37.7230	87.29	0.46	0.3776E-01
1.8190	0.3985	37.6519	87.23	0.60	0.3769E-01

C_{xx} = .9904 C_{yx} = 0.0169 C_{zx} = 0.0086

C_{xy} = 0.0013 C_{yy} = 0.0019 C_{zy} = 0.0019

C_{xz} = -0.0082 C_{yz} = 0.0074 C_{zz} = 1.0000

X, Y, Z - Magnetometer outputs for each axis

D, I - Declination, inclination relative to sample

M - Total moment (x 10^{-4} emu)

Table 2: Corrected measurements of Calibration Sample

X	Y	Z	D	I	M
3.6700	-8.0600	3.3000	155.51	20.43	0.9451E-02
3.1600	-8.0200	-3.8300	154.47	19.57	0.9432E-02
-3.8800	-7.9800	-3.3900	154.07	20.90	0.9498E-02
-3.3000	-7.9500	3.7600	154.68	20.56	0.9393E-02
3.6600	-3.2900	-8.0200	155.47	20.46	0.9409E-02
3.9000	3.3800	7.9400	153.84	20.91	0.9469E-02
8.1600	3.7400	3.3800	155.37	20.63	0.9591E-02
3.3300	3.7600	-8.0500	154.96	20.54	0.9488E-02
-8.0900	3.7300	-3.2300	155.24	19.92	0.9475E-02
-3.2600	3.7000	8.0200	155.23	20.25	0.9414E-02
8.0600	-3.3000	3.6200	155.81	20.48	0.9431E-02
8.0400	3.2800	-3.7600	154.93	20.28	0.9462E-02
-3.6100	8.1400	3.4500	156.08	21.17	0.9549E-02
3.5200	8.0700	3.8100	154.72	21.52	0.9593E-02
3.9100	8.0900	-3.3000	154.20	20.16	0.9572E-02
-3.2500	8.1400	-3.6800	155.67	19.99	0.9506E-02
-3.7000	-3.3200	8.0800	155.39	20.48	0.9486E-02
-3.7100	3.4000	-7.9600	155.01	21.16	0.9417E-02
-8.0800	-3.7500	3.3300	155.10	20.49	0.9509E-02
3.3900	-3.8000	8.0500	154.73	20.84	0.9525E-02
8.0500	-3.7600	-3.4600	154.96	21.27	0.9534E-02
-3.4900	-3.7600	-8.0000	154.82	21.54	0.9503E-02
-8.1500	-3.3100	-3.6700	155.75	20.32	0.9531E-02
-8.0200	3.3600	3.9000	154.06	20.64	0.9529E-02

Table 3: Uncorrected measurements on 2-5 cm core of fine grained basalt

X	Y	Z	D	I	M
3.7424	-7.9497	-3.3894	154.79	21.09	0.9417E-02
3.2981	-7.9241	-3.7444	154.70	20.62	0.9364E-02
-3.6788	-7.8931	-3.3619	155.01	21.10	0.9334E-02
-3.1665	-7.8495	3.7919	154.21	19.96	0.9274E-02
3.7496	-3.2594	-7.9651	154.79	20.31	0.9387E-02
3.7371	3.3582	7.9458	154.81	20.92	0.9401E-02
7.9895	3.7110	3.4181	155.08	21.20	0.9449E-02
3.3040	3.7032	-8.0502	155.29	20.44	0.9547E-02
-8.0476	3.6673	-3.3231	155.50	20.59	0.9447E-02
-3.3604	3.6649	7.9653	155.29	20.96	0.9389E-02
8.0073	-3.2419	3.7096	155.14	20.17	0.9401E-02
7.9400	3.2433	-3.7187	154.90	20.30	0.9348E-02
-3.7426	8.0413	3.3599	155.04	20.74	0.9484E-02
3.3171	7.9823	3.7783	154.67	20.58	0.9433E-02
3.7644	7.9894	-3.3280	154.77	20.64	0.9438E-02
-3.3245	8.0286	-3.7665	154.86	20.55	0.9470E-02
-3.6781	-3.2690	8.0739	155.50	20.22	0.9455E-02
-3.6632	3.3384	-8.0147	155.43	20.74	0.9423E-02
-7.9680	-3.7083	3.2919	155.04	20.53	0.9385E-02
3.3522	-3.7337	8.1050	155.26	20.58	0.9532E-02
8.0662	-3.7094	-3.3663	155.30	20.76	0.9495E-02
-3.3241	-3.7331	-7.9997	154.98	20.63	0.9433E-02
-7.9844	-3.2868	-3.7112	155.07	20.47	0.9398E-02
-8.0335	3.3151	3.8095	154.62	20.44	0.9489E-02

Table 4: Corrected results for same sample as Table 3

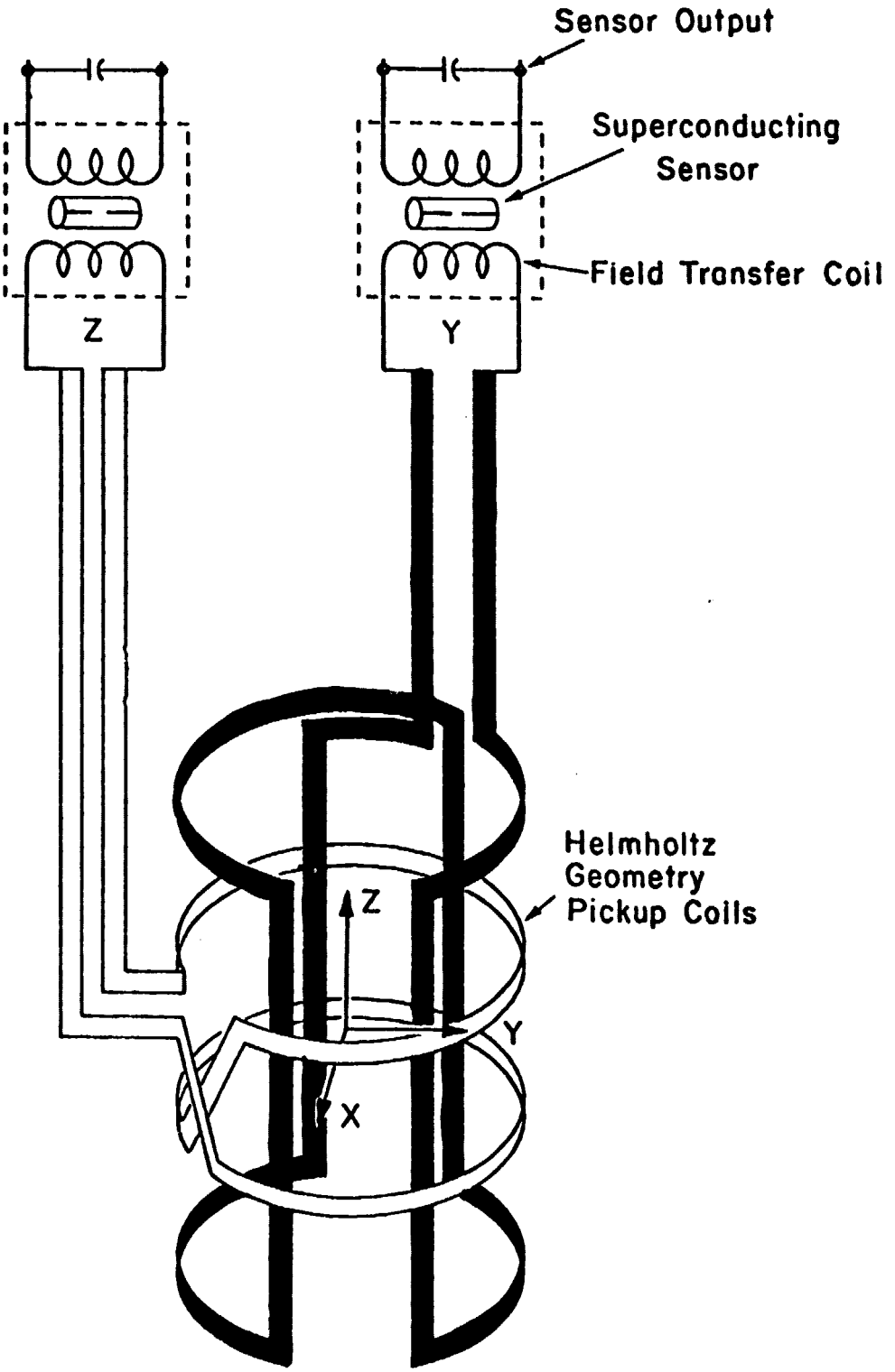

Fig. 1 SENSE COIL GEOMETRY (TWO-AXIS SYSTEM)

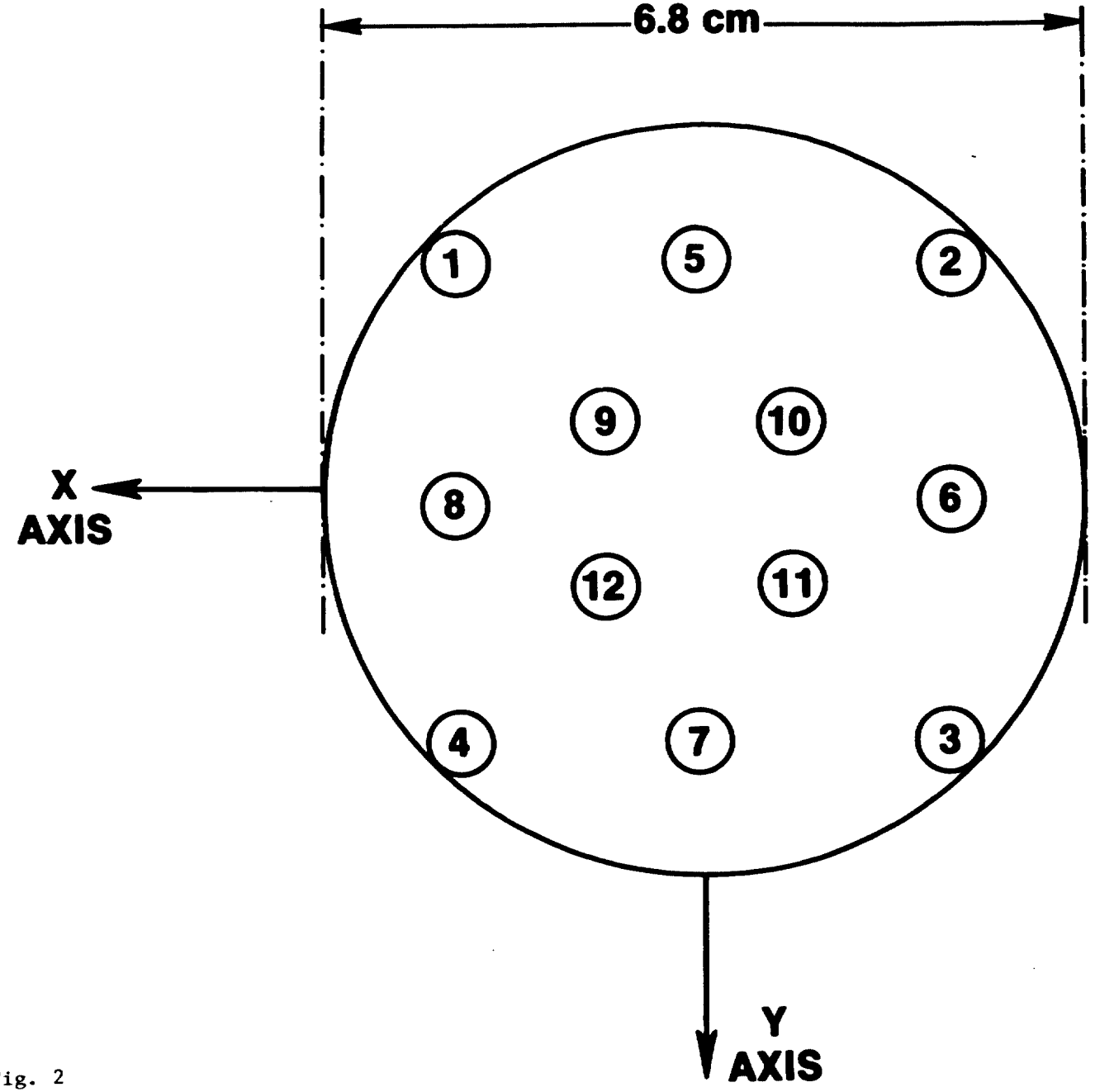

Fig. 2

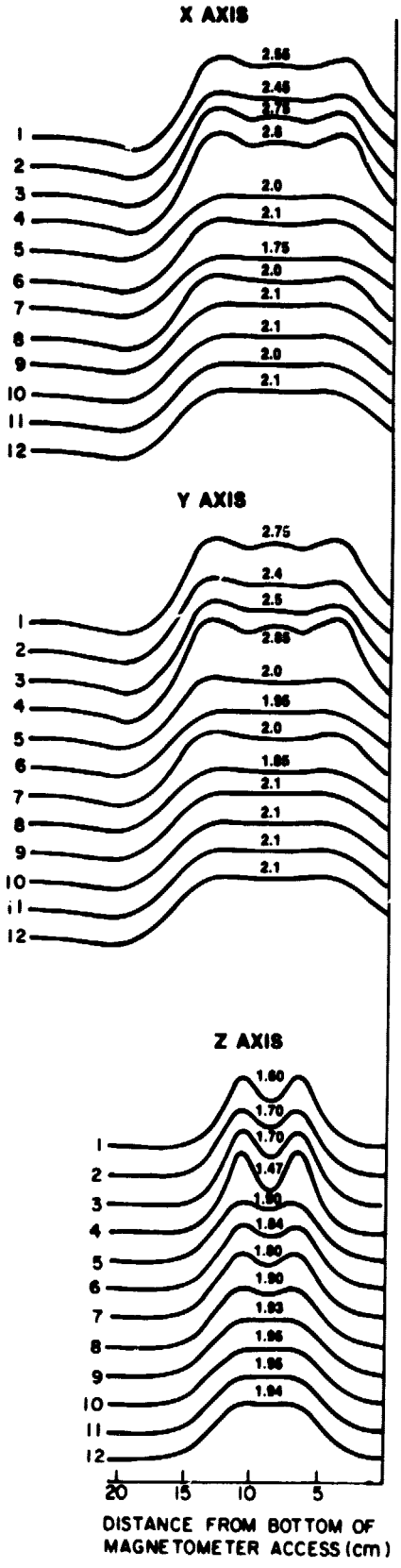
X AXIS
2.85
2.45
2.75
2.8
2.0
2.1
1.75
2.0
2.1
2.1
2.0
2.1
1
2
3
4
5
6
7
8
9
10
11
12
Y AXIS
2.75
2.4
2.5
2.85
2.0
1.95
2.0
1.85
2.1
2.1
2.1
2.1
1
2
3
4
5
6
7
8
9
10
11
12
Z AXIS
1.80
1.70
1.70
2.47
1.84
1.80
1.90
1.93
1.95
1.95
1.94
1
2
3
4
5
6
7
8
9
10
11
12
20
15
10
5
DISTANCE FROM BOTTOM OF
MAGNETOMETER ACCESS (cm)

Fig. 3

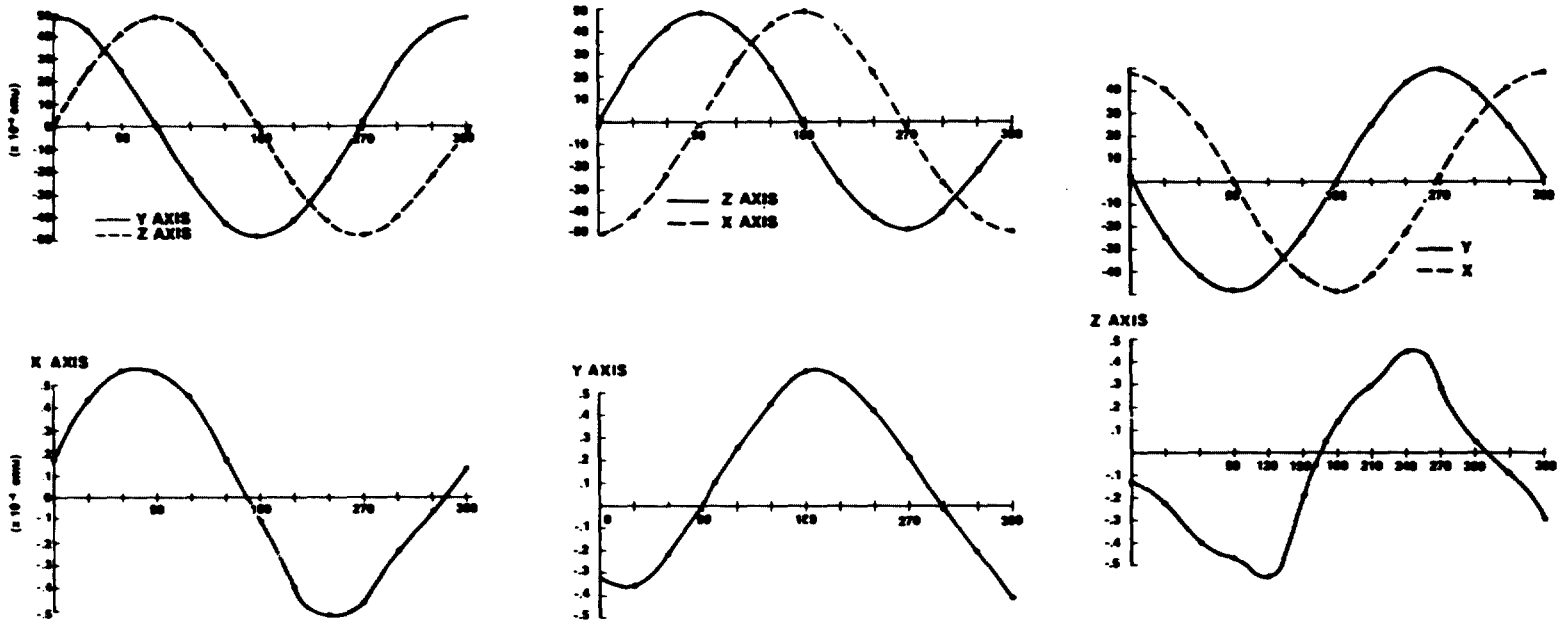

Fig. 4

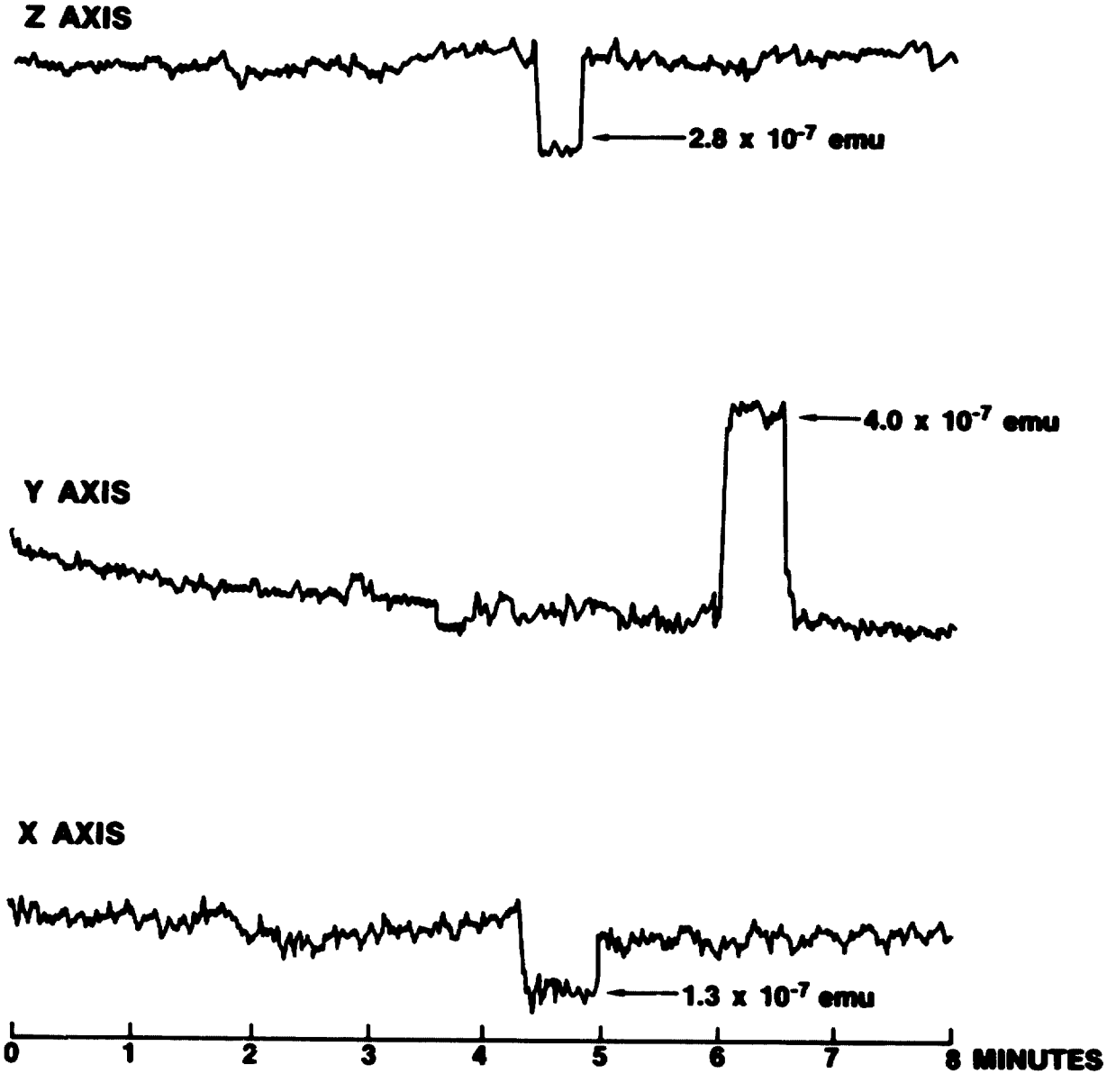
Z AXIS
2.8 x 10⁻⁷ emu
Y AXIS
4.0 x 10⁻⁷ emu
X AXIS
1.3 x 10⁻⁷ emu
0
1
2
3
4
5
6
7
8 MINUTES

Fig. 5

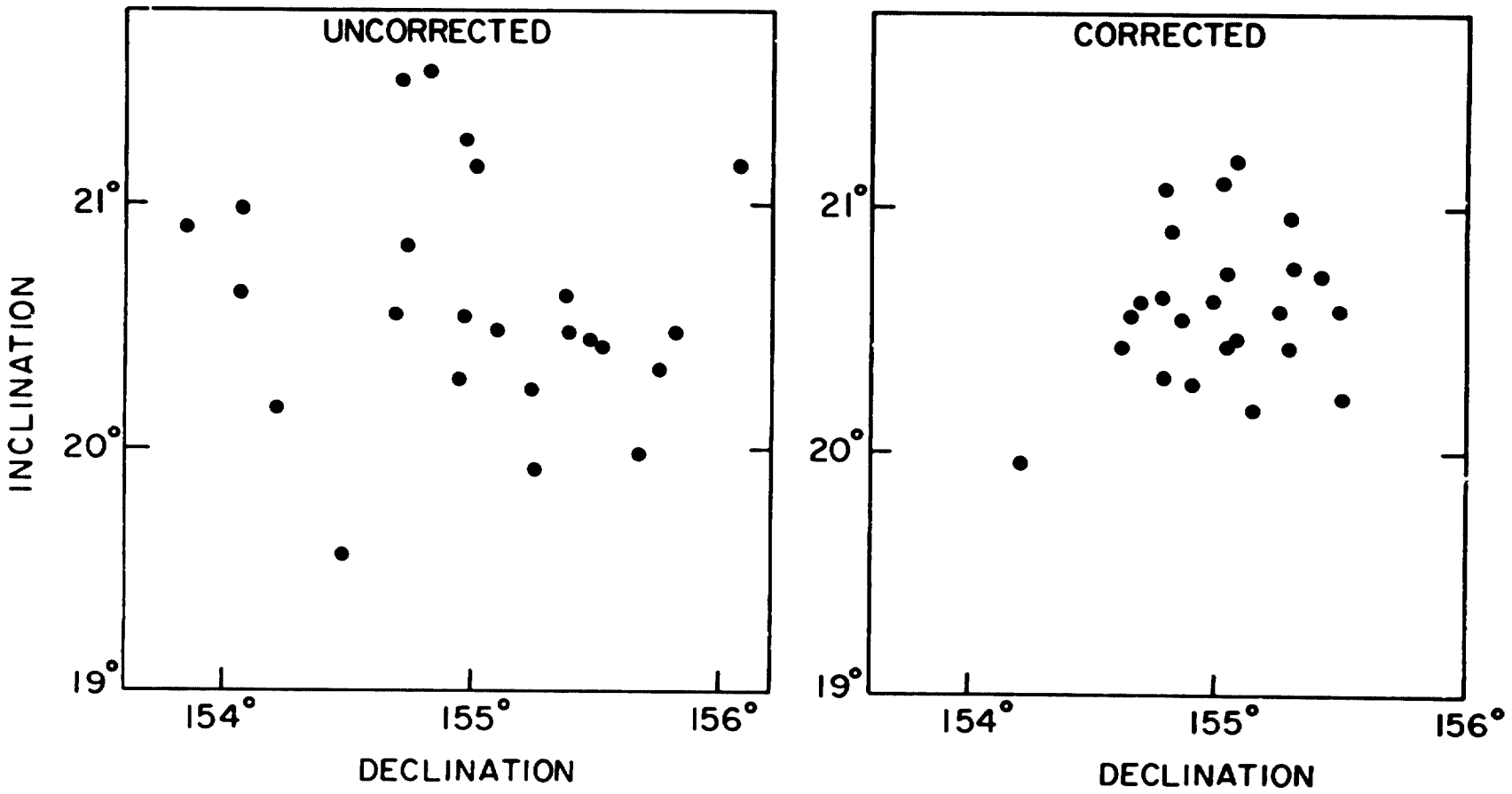
UNCORRECTED
CORRECTED
INCLINATION
21°
20°
19°
154°
155°
156°
DECLINATION

Fig. 6